PRAMANA
— journal of
physics

Vol. 79, No. 6
December 2012
pp. 1485–1493

The effect of impurity on transition frequency of bound polaron in quantum rods

WEI XIAO[1] and JING-LIN XIAO[2,*]

[1]Department of Basic, University of Informational Science and Technology of Beijing, Beijing 100101, China

[2]College of Physics and Electronic Information, Inner Mongolia National University, Tongliao 028043, China

*Corresponding author. E-mail: xiaojlin@126.com

MS received 27 November 2011; revised 25 April 2012; accepted 29 May 2012

Abstract. The Hamiltonian of a quantum rod with an ellipsoidal boundary is given after a coordinate transformation that changes the ellipsoidal boundary into a spherical one. The properties of the quantum rods constituting the bridge between two-dimensional quantum wells, zero-dimensional quantum dots and one-dimensional quantum wires are explored theoretically using linear combination operator method. The first internal excited state energy, the excitation energy and the transition frequency between the first internal excited and the ground states of the strong-coupled impurity-bound polaron in the rod with Coulomb-bound potential, the transverse effective confinement length, the ellipsoid aspect ratio and the electron–phonon coupling strength are studied. It is found that the first internal excited state energy, the excitation energy and the transition frequency are increasing functions of the Coulomb-bound potential and the electron–phonon coupling strength, whereas they are decreasing functions of the ellipsoid aspect ratio and the transverse effective confinement length. These results can be attributed to the interesting quantum size confining effects.

Keywords. Quantum rods; linear combination operator; impurity-bound polaron; aspect ratio.

PACS Nos 71.38.−k; 63.22.−m; 63.20.kd

1. Introduction

Both zero-dimensional quantum dots (QDs) and one-dimensional quantum wires (QWs) were extensively studied and utilized in electronic and optoelectronic devices owing to their unique quantum confinement properties. An interesting intermediate structure between zero- and one-dimensional confinements is represented by elongated QDs, i.e., quantum rods (QRs) [1] or nanorods. Ever since the shape-controlled colloidal QRs were realized in experiments by modifying the synthesis [2,3], it has become a hot field of investigation in quantum functional device. Consequently, there has been a large amount

of experimental work [4–6] on this device. Meanwhile, many investigators studied its properties in many aspects using a variety of theoretical methods [7–10]. Ahrenkiel *et al* [11] synthesized InP nanorods and nanowires of 30–300 Å diameter and 100–1000 Å length. The transition energy between QDs and QWs was explored theoretically by Planelles *et al* [12] using the addition energy spectra of nanorods of different lengths. Katz *et al* [13] and Htoon *et al* [14] obtained the same results. Within the femtosecond pump and probe spectroscopy, Creti *et al* [15] analysed the effect of shell thickness on stimulated emission and photo-induced absorption transitions in CdSe QRs. El Brolossy *et al* [16] used photoacoustic method to measure the optical absorption properties of as-prepared CdSe QRs. Employing scanning tunnelling microscopy technique, Talaat *et al* [17] determined the energy band gap of a series of CdSe QR having different sizes at room temperature. Their results confirmed that the band gaps of such QRs depend mainly on the width (the dimension of the electron confinement) and only slightly on the length as shown previously in the literatures. Talaat *et al* compared the experimental data based on two theoretical models, i.e., the effective mass approximation and the semiempirical pseudopotential method. The theoretical values for the energy band gap at varying radii are in agreement with the experimental results within 0.08 eV. We have studied the properties of a strong-coupling magnetopolaron in QRs using linear combination operator method [18]. The properties of the impurity-bound polaron in QRs, however, have not been studied so far by employing the linear combination operator method. Especially, the properties of the transition frequency of the impurity-bound polaron have not been investigated yet.

In this article, we investigate the effect of hydrogen-like impurity, the ellipsoid aspect ratio, the electron–phonon coupling strength and the transverse effective confinement lengths on the transition frequency of a strong-coupling impurity-bound polaron in the QRs using linear combination operator method. We also study its first excited state energy and the excitation energy as functions of the Coulomb-bound potential, the electron–phonon coupling strength, the transverse effective confinement length and the ellipsoid aspect ratio.

2. Theory model

As shown in figure 1, the electron under consideration is moving in a polar crystal QR with three-dimensional anisotropic harmonic potential, and is interacting with bulk LO phonons.

The Hamiltonian of the system with a hydrogen-like impurity at the centre can be written as

$$H = \frac{p_{\parallel}^2}{2m} + \frac{p_z^2}{2m} + \frac{1}{2}m\omega_{\parallel}^2\rho^2 + \frac{1}{2}m\omega_z^2 z^2 + \sum_{\mathbf{q}} \hbar\omega_{\mathrm{LO}} a_{\mathbf{q}}^{+} a_{\mathbf{q}} + \sum_{\mathbf{q}} \left[V_q a_{\mathbf{q}} \exp(i\mathbf{q}\cdot\mathbf{r}) + \mathrm{h{\cdot}c.} \right] - \frac{e^2}{\varepsilon_0 r}, \tag{1}$$

where m is the band mass, $\omega_{\parallel}$ and ω_z are the measures of the transverse and longitudinal confinement strengths of the three-dimensional anisotropic harmonic potential in the radius and the length directions of the rod, respectively. $a_{\mathbf{q}}^{+}(a_{\mathbf{q}})$ denotes the creation

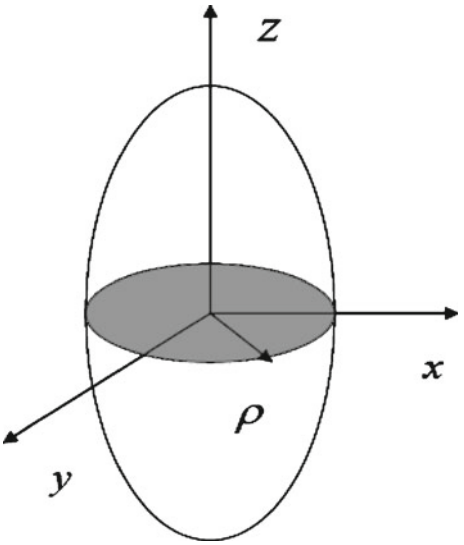

Figure 1. Schematic diagram of quantum rods.

(annihilation) operator of the bulk LO phonons with wave vector $\mathbf{q}(\mathbf{q}_\parallel, q_z)$. $\mathbf{p}(\mathbf{p}_\parallel, p_z)$ and $\mathbf{r} = (\boldsymbol{\rho}, z)$ are respectively the momentum and position vectors of the electron. $-e^2/\varepsilon_0 r$ denotes the Coulomb potential between the electron and the hydrogen-like impurity. V_q and α in eq. (1) are

$$V_q = i\left(\frac{\hbar\omega_{\mathrm{LO}}}{q}\right)\left(\frac{\hbar}{2m\omega_{\mathrm{LO}}}\right)^{1/4}\left(\frac{4\pi\alpha}{v}\right)^{1/2},$$

$$\alpha = \left(\frac{e^2}{2\hbar\omega_{\mathrm{LO}}}\right)\left(\frac{2m\omega_{\mathrm{LO}}}{\hbar}\right)^{1/2}\left(\frac{1}{\varepsilon_\infty} - \frac{1}{\varepsilon_0}\right). \tag{2}$$

Employing Fourier expansion to the Coulomb-bound potential, it can be written as

$$-\frac{e^2}{\varepsilon_0 r} = -\frac{4\pi e^2}{\varepsilon_0 v}\sum_{\mathbf{q}}\frac{1}{q^2}\exp\left(-i\mathbf{q}\cdot\mathbf{r}\right). \tag{3}$$

We introduce a coordinate transformation [7], which changes the ellipsoidal boundary into a spherical one: $x' = x$, $y' = y$, $z' = z/e'$, where e' is the ellipsoid aspect ratio and (x', y', z') is the transformed coordinate. The electron–phonon system Hamiltonian in the new coordinate is changed to H'. We then introduce a linear combination operator:

$$\begin{aligned} p_j &= \left[\frac{m\hbar\lambda}{2}\right]^{1/2}(b_j + b_j^+), \\ r_j &= i\left[\frac{\hbar}{2m\lambda}\right]^{1/2}(b_j - b_j^+), \end{aligned} \qquad j = x, y, z, \tag{4}$$

where λ is the variational parameter. Inserting eq. (4) into H' and carrying out the unitary transformation to H':

$$U = \exp\left[\sum_q (a_q^+ f_q - a_q f_q^*)\right], \tag{5}$$

where $f_q(f_q^*)$ is the variational function. The ground- and the first internal excited-state wave functions of the system are chosen as

$$|\Psi_0\rangle = |0\rangle_a |0\rangle_b , \tag{6}$$

$$|\psi_1\rangle = |0\rangle_a |1\rangle_b , \quad |1\rangle_b = b^+ |0\rangle_b , \tag{7}$$

where $|0\rangle_b$ is the vacuum state of the b operator and $|0\rangle_a$ is the unperturbed zero-phonon state.

The expectation value of H' with respect to $|\psi_0\rangle$ and $|\psi_1\rangle$ can be expressed as

$$F_0(\lambda, f_q) = \langle\psi_0| U^{-1} H' U |\psi_0\rangle , \tag{8}$$

$$F_1(\lambda, f_q) = \langle\psi_1| U^{-1} H' U |\psi_1\rangle . \tag{9}$$

Performing the variation of $F_0(\lambda, f_q)$ and $F_1(\lambda, f_q)$ with respect to λ and choosing the usual polaron unit ($\hbar = 2m = \omega_{\rm LO} = 1$), we obtain the impurity-bound polaron ground state energy E_0 and the first excited state energy E_1. The first excited state energy of the strong-coupling impurity-bound polaron in a QR can be written as

$$E_1 = \lambda_0 + \frac{3e'^2}{4}\lambda_0 + \frac{4}{\lambda_0 l_p^4} + \frac{3}{\lambda_0 l_v^4 e'^2} - \frac{2\alpha}{3\sqrt{\pi}}\sqrt{\lambda_0}A(e') - \frac{4\beta}{3}\sqrt{\lambda_0}A(e'), \tag{10}$$

where $\beta = (e^2/\varepsilon_0)\sqrt{(m/\pi\hbar)}$ is the Coulomb-bound potential. $l_p = \sqrt{\hbar/m\omega_{\|'}}$ and $l_v = \sqrt{\hbar/m\omega_{z'}}$ are the transverse and longitudinal effective confinement lengths, respectively. The excitation energy of the polaron is given by

$$\Delta E = E_1 - E_0 = \frac{\lambda_0}{2}(1 + e'^2) + \frac{2}{\lambda_0 l_p^4} + \frac{2}{\lambda_0 l_v^4 e'^2} + \frac{\alpha\sqrt{\lambda_0}}{3\sqrt{\pi}}A(e') + \frac{2\beta}{3}\sqrt{\lambda_0}A(e'). \tag{11}$$

The transition frequency between the first excited and the ground states of polaron can be expressed as

$$\omega = \frac{E_1 - E_0}{\hbar} = \frac{\lambda_0}{2}(1 + e'^2) + \frac{2}{\lambda_0 l_p^4} + \frac{2}{\lambda_0 l_v^4 e'^2} + \frac{\alpha\sqrt{\lambda_0}}{3\sqrt{\pi}}A(e') + \frac{2\beta}{3}\sqrt{\lambda_0}A(e'). \tag{12}$$

3. Numerical results and discussion

Numerical calculation results on the first excited state energy E_1, the excitation energy ΔE and the transition frequency ω of the strong-coupling impurity-bound polaron in a

QR vs. the Coulomb-bound potential β, the ellipsoid aspect ratio e', the electron–phonon coupled strength α and the transverse effective confinement length l_p are presented in figures 2–5.

Figures 2 and 3 show the relation between the first excited state energy E_1 and the transition frequency ω of the strong-coupling impurity-bound polaron varying with β for $\alpha = 6.5$, $e' = 1.4$, $l_v = 2.0$. The solid and the dotted lines correspond to the transverse effective confinement length $l_p = 2.0$ and 4.0, respectively. From the two figures we can see that E_1 and ω increase with increasing β. The reason is that there is Coulomb potential between the electron and the hydrogen-like impurity because of the existence of the impurity at the centre. Therefore, it leads to the increment of the electron energy which makes the electrons interact with more phonons. In this way E_1 and ω are increased. From another point of view, the presence of Coulomb potential is equivalent to the introduction of another new confinement on the electrons, leading to a greater overlapping of electrons' wavefunctions so that the electron–phonon interactions will be enhanced, eventually resulting in the increase of E_1 and ω. From the two figures one finds that E_1 and ω are decreasing functions of l_p. From the expression $l_p = \sqrt{\hbar/m\omega_{\|'}}$, we can see that the effective confinement length l_p is reciprocal of the square root of the confinement strength $\omega_{\|'}$, and then the first excited state energy and the transition frequency will increase with increasing confinement strength. Physically, this is because the motion of the electrons is confined by the confining potential. When the confining potential ($\omega_{\|'}$) increases, that is, when ρ' decreases, the electron energy and the interaction energy between the electrons and the phonons are enhanced because of the smaller range in particle motion. As a result, the first excited state energy and the transition frequency of the polaron are increased. From another point of view, the presence of parabolic confining potentials in the transverse radius direction of the rod is equivalent to the introduction of another new confinement on the electrons leading to the increase of E_1 and ω. These can

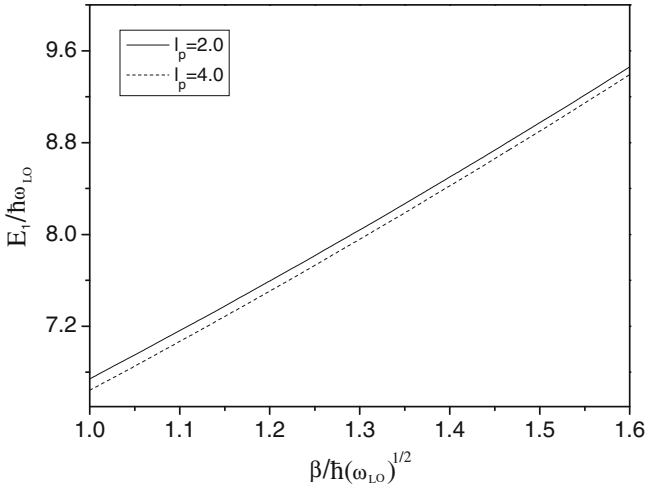

Figure 2. The relational curves of the first excited state energy E_1 with the Coulomb-bound potential β.

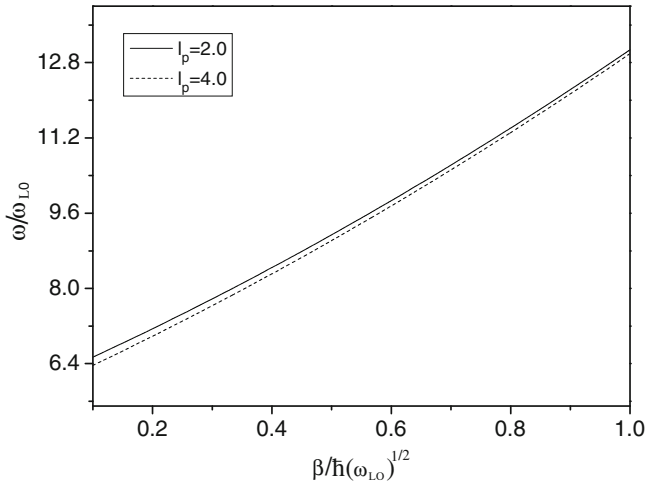

Figure 3. The relational curves of the transition frequency ω with the Coulomb-bound potential β.

also be attributed to the interesting quantum size confining effects. As the diameter of the QR corresponds to the vertical confinement length of the electrons, our result obtained by the linear combination operator method that E_1 and ω increase with decreasing l_p indicates that the confinement along the radial direction of the QR is stronger. Moreover, our result is in good agreement with that obtained in ref. [17], where they examined the band gap of the QR varying with respect to the diameter by using the effective mass approximation and the semiempirical pseudopotential method.

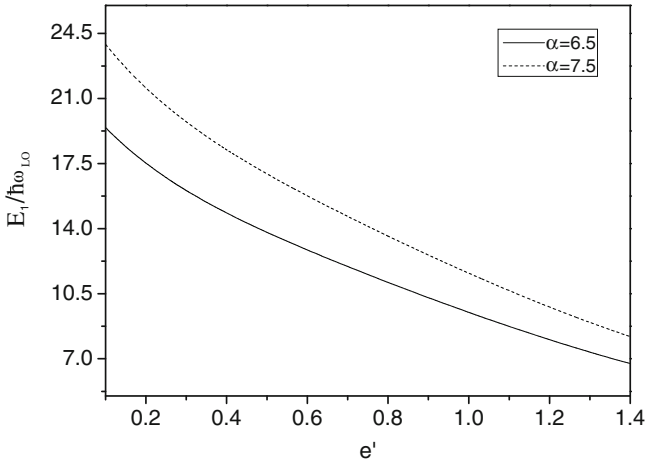

Figure 4. The relational curves of the first excited state energy E_1 with the ellipsoid aspect ratio e'.

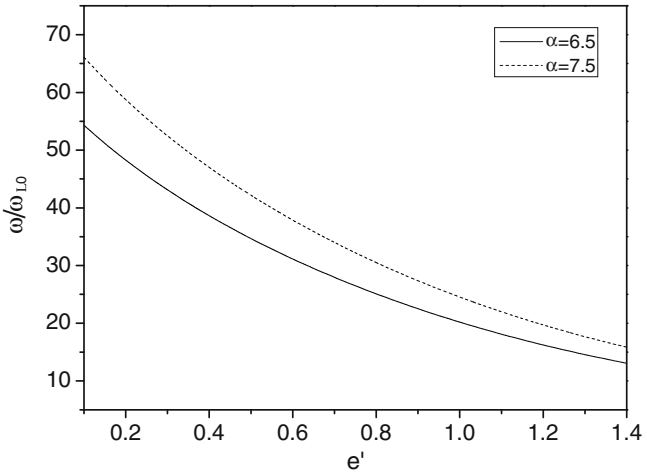

Figure 5. The relational curves of the transition frequency ω with the ellipsoid aspect ratio e'.

Figures 4 and 5 depict the first excited state energy E_1 and the transition frequency ω as functions of the ellipsoid aspect ratio e' for $\beta = 2.0$, $l_p = 4.0$ and $l_v = 2.0$. The solid and the dotted lines correspond to the electron–phonon coupled strength $\alpha = 6.5$ and 7.5, respectively. From the two figures, we can see that E_1 and ω increase with decreasing e', the aspect ratio of the ellipsoid. These results are in agreement with the results obtained in refs [7,19]. For ellipsoidal QRs $e' = L/2R$, where L and $2R$ are the longitudinal length and the transverse diameter of the rod, respectively. By increasing e', that is, by increasing the longitudinal length L of the rod, the electron energy and the electron–phonon coupled energy decrease because of the larger motion space of the electron. As a result, E_1 and ω decrease with increasing e'. This result is similar to the case of QW obtained in ref. [12]. Conversely, with the decrease in the aspect ratio e', the electron energy and the electron–phonon coupled energy are enhanced because of the smaller electron motion space. Correspondingly, E_1 and ω are increased due to the interesting quantum size confining effects. This result is also similar to the case of the quantum well in ref. [20]. This indicates that when the aspect ratio is quite small, the shape of the rod approaches a two-dimensional quantum well. At the extreme case, when the aspect ratio equals 1, the rod becomes a zero-dimensional QD. If the aspect ratio is large enough, the rod resembles a one-dimensional QW. In other words, QRs constitute the bridge between two-dimensional quantum wells, zero-dimensional QDs and one-dimensional QWs. Investigations of the transition regime from quantum wells to QDs and to QWs are of particular interest in the case of colloidal semiconductor QRs because size and shape controls enable the synthesis of QRs with precise length and diameter. Therefore, by tuning the aspect ratio of the ellipsoid one can follow the transition from two- to zero-, and to one-dimensional systems. This property offers an opportunity for designing new quantum devices. Results in refs [12–14] indicated that the QRs constitute the bridge between QDs and QWs, whereas our results indicate that the QRs constitute a bridge between all the above three low-two-dimensional structures. We can also see that E_1 and ω are increasing functions of

the electron–phonon coupled strength α because the larger the electron–phonon coupling strength is, the stronger is the electron–phonon interaction. Therefore, it leads to the electron energy increment and makes the electrons interact with more phonons. In this way the first excited state energy and the transition frequency are increased. It is known that the electron–phonon interaction strength α is different in different crystal materials, and then the first excited state energy and the transition frequency can be tuned by changing α. In quantum bit, the electron–phonon interaction strength will be increased when the system is confined, resulting in larger transition frequency and destruction of the superposition state (decoherence) [21,22]. The present result of controlling the superposition state by tuning ground state and first excited state may have practical applications in quantum information processes.

From the expressions of eqs (11) and (12), we can see that the relationships between the transition frequency of the strong-coupling impurity-bound polaron in a quantum rod varying with the Coulomb bound potential, the ellipsoid aspect ratio, the electron–phonon coupling strength and the transverse effective confinement length are all the same as the excitation energy.

4. Conclusion

The transition energy between two-dimensional quantum wells, zero-dimensional quantum dots and one-dimensional quantum wires is explored theoretically. Based on the linear combination operator method, we have investigated the first excited state energy, the excitation energy and the transition frequency between the first excited and the ground states of a strong-coupling impurity-bound polaron in a quantum rod. It is found that these three quantities increase with increase in the Coulomb-bound potential. They are increasing functions of the electron–phonon coupling strength and decreasing functions of the transverse effective confinement length and the ellipsoid aspect ratio.

Acknowledgement

This project was supported by the National Science Foundation of China under Grant No. 10964005.

References

[1] L H Li, G Patriarche, E H Linfield, S P Khanna and A G Davies, *J. Appl. Phys.* **108**, 103522 (2010)
[2] J T Hu, L S Li, W D Yang, L Manna, L W Wang and A P Alvisatos, *Science* **292**, 2060 (2001)
[3] S H Kan, T Mokari, E Rothenberg, E Rothenberg and U Banin, *Nature (London)* **2**, 155 (2003)
[4] G Sek, P Podemski, J Misiewicz, L H Li, A Fiore and G Patriarche, *Appl. Phys. Lett.* **92**, 021901 (2008)
[5] B Bruhn, J Valenta and J Linnros, *Nanotechnol.* **20**, 505301 (2009)
[6] F Ratto, P Matteini, F Rossi and R Pini, *J. Nanopart. Res.* **12**, 2029 (2010)
[7] X Z Li and J B Xia, *Phys. Rev.* **B66**, 115316 (2002)
[8] F Comas, N Studart and G E Marques, *Solid State Commun.* **130**, 477 (2004)

[9] Z X Sun, I Swart, C Delerue, D Vanmaekelbergh and P Liljeroth, *Phys. Rev. Lett.* **102**, 196401 (2009)
[10] J L Xiao and C L Zhao, *J. Low. Temp. Phys.* **163**, 302 (2011)
[11] S P Ahrenkiel, O I Micic, A Miedaner, C J Curtis, J M Nedeljkovic and A J Nozik, *Nano. Lett.* **3**, 833 (2003)
[12] J Planelles, M Royo, A Ballester and M Pi, *Phys. Rev.* **B80**, 045324 (2009)
[13] D Katz, T Wizansky, O Millo, E Rothenberg, T Mokari and U Banin, *Phys. Rev. Lett.* **89**, 086801 (2002)
[14] H Htoon, J A Hollingsworth, R Dickerson and V I Klimov, *Phys. Rev. Lett.* **91**, 227401 (2003)
[15] A Creti, M Z Rossi, G Lanzani, M Anni, L Manna and M Lomascolo, *Phys. Rev.* **B73**, 165410 (2006)
[16] T A El-Brolossy, S Abdallah, T Abdallah, H Awad, M B Mohamed, S Negm and H Talaat, *Eur. Phys. J. Special Topics* **153**, 369 (2008)
[17] H Talaat, T Abdallah, M B Mohamed, S Negm and M A El-Sayed, *Chem. Phys. Lett.* **473**, 288 (2009)
[18] J L Xiao and C L Zhao, *Superlatt. Microstruct.* **49**, 9 (2011)
[19] J B Li and L W Wang, *Nano. Lett.* **3**, 101 (2003)
[20] S S Li and J B Xia, *Appl. Phys. Lett.* **92**, 022102 (2008)
[21] Z W Wang and J L Xiao, *Acta. Phys. Sin.* **56**, 678 (2007)
[22] H J Li, J K Sun and J L Xiao, *Chin. Phys.* **B19**, 010314 (2010)